JOC The Journal of Organic Chemistry

Article

pubs.acs.org/joc

Identification of Palytoxin–Ca^{2+} Complex by NMR and Molecular Modeling Techniques

Patrizia Ciminiello, Carmela Dell'Aversano, Emma Dello Iacovo, Martino Forino,* Antonio Randazzo, and Luciana Tartaglione

Department of Pharmacy, University of Napoli "Federico II", Italy Via D. Montesano, 49-80131 Napoli, Italy

Supporting Information

ABSTRACT: More than 40 years after its isolation, the understanding of how palytoxin interacts with biological systems has yet to be fully determined. The Na^+,K^+-ATPase pump constitutes a molecular receptor for palytoxin that is able to convert the pump into an open channel, with consequent loss of cellular K^+ and remarkable rise of cytosolic Na^+ levels. In addition, a slight permeability to Ca^{2+} is detected when palytoxin binds to the pump. It has been demonstrated that the increase of cytosolic free Ca^{2+} concentration gives rise to downstream events ultimately leading to cell death. The widely accepted recognition of the dependence of important cellular events on calcium ion concentration propelled us to investigate the occurrence of palytoxin–Ca^{2+} complex in aqueous solution by NMR- and molecular modeling-based approach. We identified two specific regions of palytoxin where Ca^{2+} is preferentially coordinated. This study constitutes the first characterization of a calcium complex with palytoxin and, as such, is expected to support the investigation of the toxin molecular bioactivity.

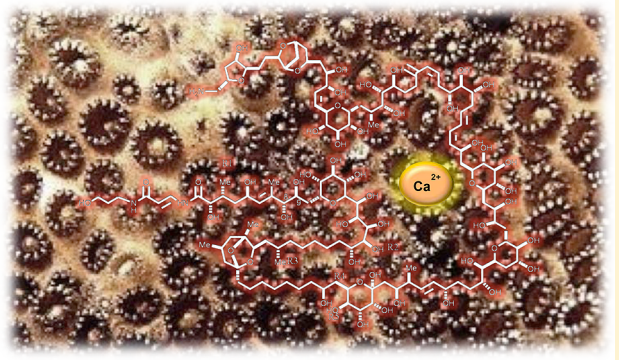

INTRODUCTION

Palytoxin (Figure 1) ranks among the most poisonous nonprotein natural toxins so far known. Since its isolation in 1971,[1] the scientific interest in palytoxin has never faded away. Numerous studies have in fact been performed on palytoxin with the purpose of investigating its chemistry, detection in the environment, ecobiology, and biogenetic origin as well as its metabolism, mechanism of action, and toxicology. Nonetheless, some aspects relative to this intriguing toxin, such as its interaction with biological systems, still remain poorly understood. It has been proven that palytoxin is capable of altering the mechanisms of ion homeostasis in both excitable and nonexcitable tissues[2,3] by binding to the plasmalemmal Na^+,K^+-ATPase pump.[4] The binding of palytoxin to the external side of the enzyme converts the pump into an open channel, with consequent loss of cellular K^+ and remarkable rise of cytosolic Na^+ levels. In addition, a slight permeability to Ca^{2+} is even detected when palytoxin binds to the pump.[5] In bovine aortic endothelial cells, the increase of cytosolic free Ca^{2+} concentration ($[Ca^{2+}]_i$) gives rise to downstream events ultimately leading to cell death.[6]

On account of the widely accepted recognition of the dependence of important cellular events on calcium ion concentration, we investigated the possible occurrence of palytoxin–Ca^{2+} complex in aqueous solution, following the MS-based observation that palytoxin possesses high affinity for divalent cations.[7] In this MS-driven study, the presence of triply charged adducts ions of palytoxin ($[M + H + Ca]^{3+}$, $[M + H + Mg]^{3+}$, and $[M + H + Sr]^{3+}$, respectively) versus the doubly charged ones in the full MS spectrum was found to be enhanced upon addition of divalent cations to a palytoxin sample. Among the tested cations (Ca^{2+}, Mg^{2+}, and Sr^{2+}), palytoxin showed the highest affinity specifically for calcium.[7]

RESULTS AND DISCUSSION

A putative palytoxin was extracted from samples of *Palythoa* spp. and purified as reported in the Experimental Section. Due to the high complexity of the molecule, it was crucial to ascertain that the purified molecule was in fact palytoxin and not a possible structural- and/or stereoisomer. Therefore, an extensive homo- and heteronuclear NMR investigation (Supporting Information, 1a–f) was carried out on the purified toxin solubilized in CD_3OD. Deuterated methanol was selected as a solvent, since a complete NMR assignment of the palytoxin stereostructure, supported also by synthetic studies, was available in the literature.[8,9] By cross-interpreting ^1H–^1H COSY and z-TOCSY, all of the toxin's spin systems were identified (Supporting Information, 1b,c). The HSQC experiment was instrumental for associating every proton to the carbon it was bonded to (Supporting Information, 1e). Finally, HMBC correlations led to identification of all of the quaternary carbons and to connect the molecule spin systems with each other (Supporting Information, 1f). This NMR-based analysis

Received: October 14, 2013
Published: December 12, 2013

   dx.doi.org/10.1021/jo4022953 | J. Org. Chem. 2014, 79, 72–79

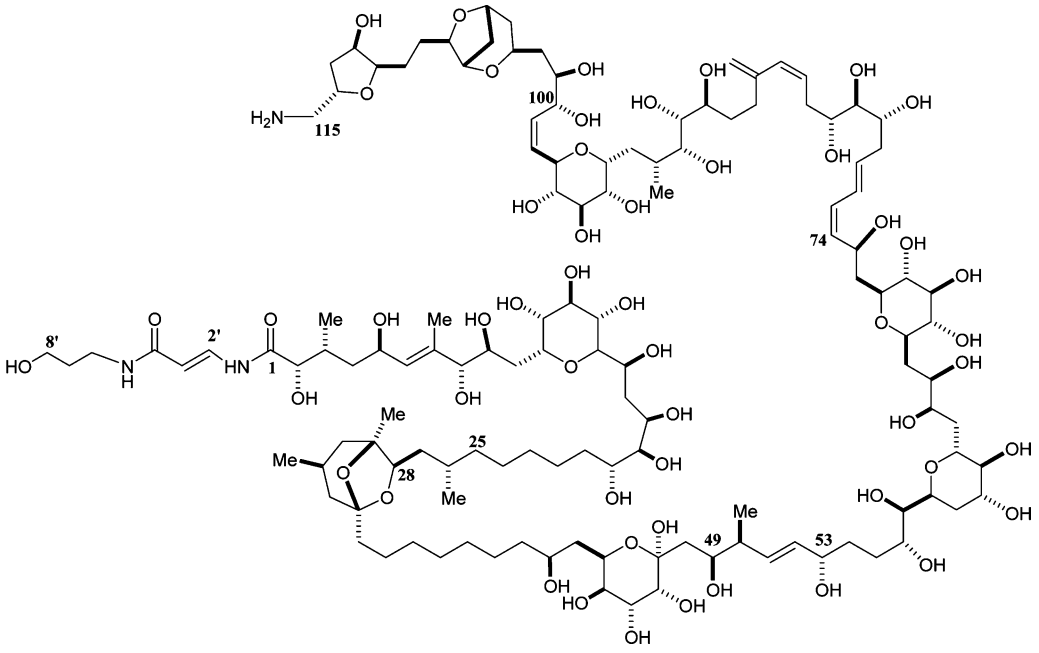

Figure 1. Stereostructure of palytoxin.

provided a complete NMR characterization of the toxin in CD_3OD that turned out totally superimposable with that reported in literature.[8,9] Thus, the purified molecule was unambiguously identified as palytoxin.

The palytoxin sample was then dried and solubilized in deuterium oxide, and a full homo- and heteronuclear NMR analysis was carried out anew (Table 1). In the literature, only the ^{1}H NMR assignment of palytoxin in D_2O has been reported this far.[10] However, some of palytoxin's proton chemical shifts we detected turned out different from those reported in previous studies.[10] Additionally, on account of the molecule size we ran both NOESY and ROESY experiments, but none of the selected dipolar couplings reported by Inuzuka et al. appeared in our spectra.[10] We hypothesized that such discrepancies might be due to the fact that under our aqueous experimental conditions palytoxin does not assume the same conformation as that described by Inuzuka et al.[10,11]

Finally, the absence of long-range NOEs, which are crucial for investigating the conformational behavior of a molecule the size of palytoxin, caused us to desist from proposing a molecular modeling-based tridimensional structure for our toxin.

Once the NMR assignment in deuterium oxide was completed, the palytoxin sample was divided into three fractions of about 1 mg each. The three obtained samples were solubilized in deuterium oxide and each transferred into an NMR tube. The first of the three samples was kept as a plain solution of palytoxin, the second was added with an excess of $CaCl_2$, and the third one was incubated with an excess of standard EDTA (8 equiv). Each of these three samples was subjected to ^{1}H NMR (Supporting Information, 2a, 3a, 4a), COSY, z-filtered TOCSY (Supporting Information, 2b, 3b, 4b), NOESY (Supporting Information, 2c, 3c, 4c), ROESY (Supporting Information, 2d, 4d), HSQC (Supporting Information, 2e), and ps-HMBC (Supporting Information, 2f) over the next 48 h, after one week and finally after two weeks.

Spectral properties of the plain solution of palytoxin appeared unaffected during each round of NMR experiments. Likewise, the NMR data obtained for palytoxin added with $CaCl_2$ over the next 48 h since the addition of the salt, after one and again after two weeks from the preparation of the sample, did not reveal any difference in comparison with those recorded for the sample of plain palytoxin.

Hence, it was hypothesized that either palytoxin was not coordinating any calcium ions or that a palytoxin−calcium complex was pre-existent to the addition of $CaCl_2$.

This was clarified by the analysis of the NMR experiments performed on the palytoxin sample added with an excess of standard EDTA.

The NMR experiments acquired over the following 48 h from the addition of standard EDTA to palytoxin were found to be superimposable on those recorded on the plain palytoxin sample. Instead, in the ^{1}H NMR spectrum, recorded after one week from the addition of EDTA, isolated proton resonances appeared to be no more superimposable with those contained in the ^{1}H NMR spectrum of palytoxin itself. By way of example, in the palytoxin's ^{1}H NMR spectrum, the H115b resonance appeared as a doublet of doublets with a large $^2J_{H-H}$ of 13.3 Hz and a small $^3J_{H-H}$ of 2.8 Hz (Figure.2). The same proton after one week of incubation with EDTA was seemingly resonating as a triple doublet of doublets (Figure.2). Due to the proton connectivity of H115b, such multiplicity had no rationale. So, it was interpreted as the sum of two doublets of doublets resonating close enough to partly overlap thus shaping into a phony triple doublet of doublets. This reasonably implied that, after one week from its addition, EDTA had partially sequestered calcium ions from palytoxin. This caused a certain percentage of palytoxin molecules to assume a different preferential conformation from that assumed when coordinating calcium ions.

One more week later, the H115b NMR signal was again resonating as a doublet of doublets but at a slightly lower chemical shift in comparison to that of palytoxin itself (Figure 2; Table 1).

dx.doi.org/10.1021/jo4022953 | J. Org. Chem. 2014, 79, 72−79

Table 1. Chemical Shift Data in D_2O of Palytoxin and Palytoxin in a Mixture with 8 equiv of Standard EDTA

	palytoxin		palytoxin + EDTA			palytoxin		palytoxin + EDTA	
position	^{13}C	^{1}H	^{13}C	^{1}H	position	^{13}C	^{1}H	^{13}C	^{1}H
1	174.67		174.62		60	70.18	3.76	70.20	3.76
2	73.79	4.06	73.72	4.06	61	73.42	3.05	73.46	3.05
3	32.44	1.99	32.36	1.99	62	70.70	3.67	70.71	3.67
Me-3	12.37	0.73	12.06	0.73	63	34.69	1.67	34.66	1.67
							1.98		1.97
4	39.25	1.31 1.63	39.08	1.31	64	70.05	3.61	69.97	3.61
				1.62					
5	64.81	4.42	64.67	4.41	65	70.05	3.60	70.00	3.60
6	130.16	5.34	130.01	5.34	66	34.56	1.36	34.52	1.35
							1.91		1.91
7	136.86		136.68		67	75.19	3.33	75.23	3.32
Me-7	11.11	1.56	11.26	1.56	68	73.42	3.06	73.50	3.06
8	78.97	3.82	78.88	3.82	69	76.78	3.32	76.80	3.33
9	69.20	3.71	69.33	3.72	70	73.42	3.05	73.50	3.06
10	27.28	1.59	27.15	1.58	71	75.24	3.31	75.16	3.31
		1.95		1.95					
11	73.58	4.07	73.55	4.07	72	38.38	1.40	38.45	1.40
							1.95		1.96
12	72.47	3.55	72.44	3.56	73	63.22	4.69	63.21	4.68
13	70.40	3.47	70.49	3.47	74	130.50	5.27	130.42	5.28
14	70.40	3.62	70.36	3.62	75	129.34	5.98	129.39	5.98
15	71.14	3.47	71.10	3.47	76	126.91	6.33	127.00	6.33
16	71.01	3.88	70.93	3.89	77	132.48	5.70	132.46	5.70
17	71.01	3.87	71.00	3.87	78	36.04	2.25	36.12	2.25
18	70.40	3.67	70.52	3.66	79	69.30	3.77	69.33	3.76
19	70.68	3.76	70.66	3.77	80	74.44	3.24	74.50	325
20	69.30	3.67	69.21	3.66	81	70.71	3.62	70.67	3.62
21	24.24	1.29	24.12	1.29	82	31.40	2.31	31.32	2.31
		1.32		1.31			2.49		2.49
22	24.70	1.39	24.58	1.38	83	128.04	5.53	128.02	5.53
		1.45		1.45					
23	34.59	1.57	34.56	1.56	84	131.29	5.87	131.31	5.87
24	28.35	1.36	28.29	1.37	85	144.61		144.57	
25	37.30	1.06	37.43	1.08	85′	113.71	4.84	113.65	4.83
		1.12		1.10			4.98		4.98
26	27.41	1.43	27.38	1.45	86	31.88	2.10	32.01	2.10
							2.16		2.16
Me-26	17.73	0.74	17.65	0.73	87	30.50	1.46	30.36	1.46
							1.58		1.57
27	37.88	0.80	37.43	0.77	88	71.88	3.59	71.90	3.59
		1.31		1.29					
28	78.46	3.94	78.30	3.92	89	72.18	3.43	72.21	3.43
29	81.32		81.22		90	75.37	3.30	75.34	3.31
Me-29	19.24	1.06	19.23	1.05	91	31.13	1.67	31.12	1.67
30	43.21	1.02	43.18	1.01	**Me-91**	13.70	0.76	13.60	0.75
		1.61		1.62					
31	23.20	1.85	23.16	1.86	**92**	25.30	1.18	25.24	1.18
							1.98		1.98
Me-31	20.04	0.76	19.94	0.76	93	72.94	4.00	73.03	4.00
32	41.44	0.98	41.46	0.97	**94**	70.76	3.62	70.73	3.62
		1.58		1.56					
33	110.10		110.00		95	71.93	3.53	71.90	3.53
34	24.36	1.67	24.30	1.67	96	73.71	3.15	73.74	3.15
35	24.36	1.46	24.30	1.46	97	67.57	4.12	67.59	4.13
36	28.46	1.18	28.44	1.18	98	130.11	5.46	130.20	5.47
37	28.46	1.18	28.44	1.18	99	134.02	5.61	133.98	5.62
38	28.46	1.18	28.44	1.18	100	70.28	4.17	70.24	4.17
39	28.13	1.37	27.97	1.37	101	69.60	3.50	69.61	3.49
40	37.94	1.44	37.87	1.45	**102**	37.81	1.42	37.93	1.42

dx.doi.org/10.1021/jo4022953 | J. Org. Chem. 2014, 79, 72−79

Table 1. continued

position	palytoxin		palytoxin + EDTA		position	palytoxin		palytoxin + EDTA	
	^{13}C	^{1}H	^{13}C	^{1}H		^{13}C	^{1}H	^{13}C	^{1}H
							1.47		1.47
41	66.97	3.73	66.85	3.74	103	66.81	4.04	66.77	4.04
42	38.21	1.35	38.32	1.33	**104**	38.86	1.31	38.96	1.31
		1.73		1.73			1.63		1.63
43	64.15	4.22	63.89	4.23	105	74.40	4.47	74.35	4.46
44	71.91	3.67	71.56	3.68	**106**	34.55	1.66	34.53	1.66
							1.76		1.76
45	71.60	3.93	71.80	3.93	107	77.75	4.16	77.66	4.16
46	67.18	3.69	67.34	3.70	108	80.93	4.24	80.85	4.24
47	100.95		101.03		109	29.74	1.35	29.84	1.36
48	37.97	1.69	38.16	1.70	**110**	24.05	1.50	23.96	1.50
		1.70		1.71			1.59		1.60
49	70.26	3.83	70.27	3.81	111	81.58	3.77	81.61	3.77
50	41.68	2.19	41.63	2.17	112	71.27	4.19	71.27	4.20
Me-50	14.75	0.88	14.62	0.87	**113**	37.24	1.81	37.16	1.81
							2.04		2.04
51	133.68	5.50	133.57	5.48	114	72.73	4.28	72.69	4.29
52	132.20	5.41	132.45	5.39	115	42.47	2.89	42.46	2.89
							3.00		2.99
53	72.04	3.98	71.86	3.97	2′	132.57	7.56	132.44	7.55
54	32.44	1.47	32.40	1.46	3′	105.78	5.81	105.73	5.81
		1.61		1.61					
55	24.78	1.30	24.74	1.30	4′	168.26		168.21	
		1.41		1.40					
56	70.57	3.66	70.62	3.66	6′	35.72	3.18	35.74	3.18
57	68.94	3.87	69.00	3.88	7′	30.53	1.63	30.49	1.62
58	71.11	3.87	70.96	3.87	8′	58.63	3.48	58.64	3.48
59	30.76	1.57	30.73	1.56					
		2.13		2.12					

Subsequent ^{1}H NMR spectra run over the following two weeks on a daily basis were found to be totally superimposable. This suggested that the calcium-free palytoxin was eventually predominant in solution. This phenomenon was detected also for other isolated proton resonances (Table 1). However, more sensible and widespread variations in terms of chemical shifts (≥0.02 ppm) were essentially limited to two specific regions of the molecule, namely the segments stretching from C25 to C33 and from C47 to C53 (Table 1). In more detail, in the z-TOCSY experiment, the correlation peak between H28 and Me-26 in palytoxin without EDTA, and therefore while coordinating calcium, resonated as a single and well-defined cross-peak (Supporting Information, 5a). In the z-TOCSY of palytoxin run after 1 week from the addition of EDTA, a new cross-peak, at slightly lower chemical shift, had appeared beside the one detected in the spectrum of palytoxin without EDTA (Supporting Information, 5b). After 2 weeks of incubation with EDTA, this new z-TOCSY cross-peak had grown more intense at the expense of the former (Supporting Information, 5c). Likewise, after 2 weeks from the addition of EDTA, the HSQC cross-peaks relative to both Me-26 and Me-50 emerged no more as single and well-defined correlations. Indeed, at lower proton and carbon chemical shifts new and much more intense HSQC cross-peaks assigned to Me-26 and Me-50, respectively, were detected alongside the ones only appearing in the HSQC spectrum of palytoxin without EDTA (Supporting Information, 6a–d).

The above NMR studies supported the hypothesis that EDTA had sequestered Ca^{2+}, thus causing palytoxin to assume a calcium-free conformation.

Conclusive proof that palytoxin had undergone sensible conformational changes in the presence of EDTA specifically along the C25–C33 and C47–C53 segments came from the analysis of some key dipolar couplings. NOESY and ROESY experiments were acquired for palytoxin without EDTA as well as for palytoxin added with the 8 equiv of EDTA after 1 week and again after 2 weeks from the addition of EDTA. Attentive comparison of the three NOESY spectra as well as of the three ROESY experiments allowed us to determine that they were all nearly superimposable apart from two sets of NOEs (or ROEs) limited again to the C25–C33 and C47–C53 segments. In particular, H28 in the palytoxin's NOESY and ROESY without EDTA appeared dipolarly coupled to both H31 and Me-26 (Figure.3a; SI 7a); after 1 week from the addition of EDTA, palytoxin's H28 was still dipolarly coupled to H31 but the intensity of the H28/Me-26 NOE/ROE was appreciably decreased (Supporting Information, 7b). One week later, H28 turned out dipolarly coupled only to H31 (Supporting Information, 7c).

Likewise, along the C47–C53 segment, palytoxin's H49 showed NOEs and ROEs with H50 and Me-50 (Figure 3b); at the same time H52 was dipolarly coupled to H50 (Figure.3b; Supporting Information, 8a,b). In both the NOESY and ROESY acquired after two weeks from the addition of EDTA, H49 was still coupled to H50 but no longer to Me-50 (Supporting Information, 8c,d); on the other hand, H52

dx.doi.org/10.1021/jo4022953 | J. Org. Chem. 2014, 79, 72–79

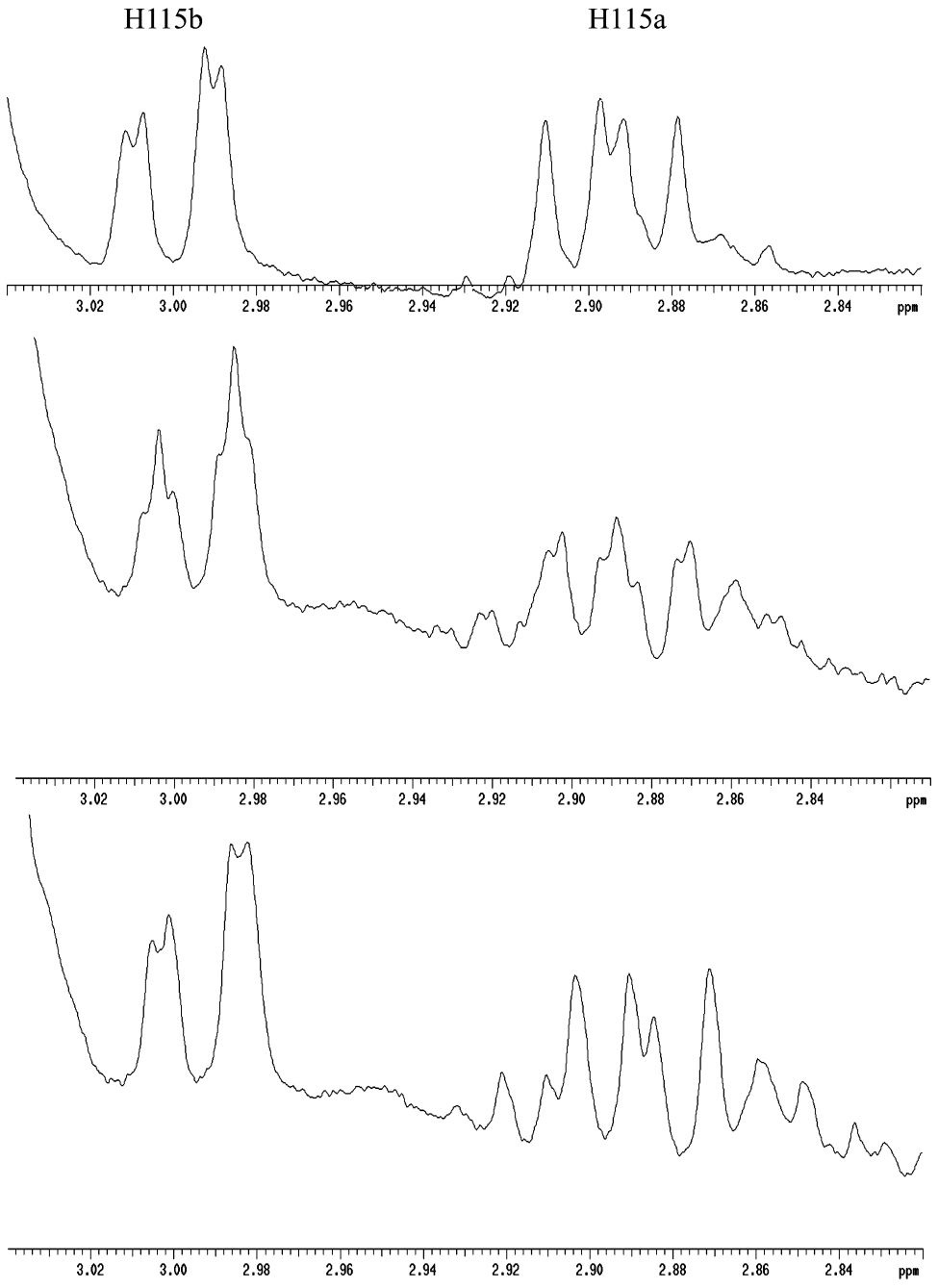

Figure 2. NMR multiplicity of H115a and H115b in palytoxin (top), palytoxin after 1 week of incubation with 8 equiv of EDTA (center), and palytoxin after 2 weeks of incubation with 8 equiv of EDTA (bottom).

appeared still coupled to H50 but also to H49 (Figure 3c; Supporting Information, 8d).

Further NMR-based evidence of the conformational changes underwent by palytoxin in the presence of EDTA along the C47−C53 segment was derived from the analysis of the coupling constants relative to H51 NMR resonance. The NMR signal of this proton in palytoxin resonated as a doublet of doublets ($^3J_{H50-H51}$= 7.1 Hz; $^3J_{H51-H52}$= 15.2 Hz), while after 2 weeks of incubation with EDTA it featured a higher $^3J_{H50-H51}$ (8.2 Hz) while keeping unaffected $^3J_{H51-H52}$. (Supporting Information, 9a,b).

In conclusion, the whole of the above NMR data led us to propose two possible palytoxin's regions, namely the C25−C33 and C47−C53 segments, where calcium ions are preferentially coordinated.

In order to get a more precise picture of the palytoxin−Ca^{2+} complex at atomic level, NOE restrained structural calculations were performed.

Heavy NMR signal overlap along with the apparent absence of long-range NOEs and ROEs as well prevented a full characterization of the three-dimensional structure of the complex. Nonetheless, insightful details on the binding of Ca^{2+} to palytoxin were obtained, by focusing the molecular modeling investigation on the two parts of the molecule mainly involved in the binding of calcium, namely C25−C33 and C45−C53 segments. Accordingly, two 3D models of the above-mentioned fragments were built. The two models included

dx.doi.org/10.1021/jo4022953 | J. Org. Chem. 2014, 79, 72−79

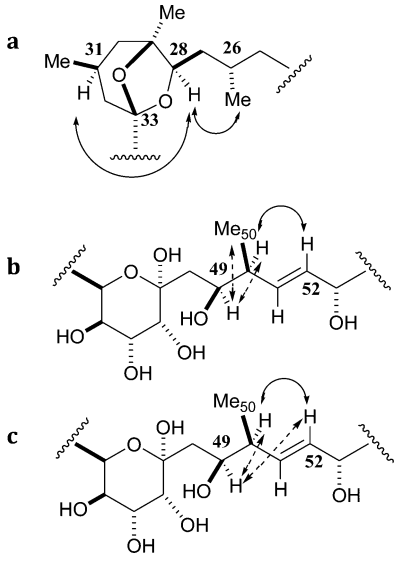

Figure 3. (a) Palytoxin C24−C34 segment. Arrows indicate key NOEs/ROEs. Me-26/H28 NOE is no longer detected in palytoxin after 2 weeks of incubation with 8 equiv of EDTA. (b, c) Palytoxin C42−C54 segment. Arrows indicate NOEs/ROEs detected in palytoxin (b) and NOEs/ROEs detected in palytoxin after 2 weeks of incubation with 8 equiv of EDTA (c).

atoms from position 21 to position 39 (fragment 1) and from position 33 to position 65 (fragment 2), respectively. Both models were subjected to restrained dynamics and mechanics calculations. In both cases, an estimation of proton−proton distances was retrieved from cross-peak intensities in 2D NOESY experiments. All distances were clustered in three groups: strong NOEs ($1.0 < r_{ij} < 3.0$ Å), medium NOEs ($2.5 < r_{ij} < 4.5$ Å) and weak NOEs ($4.0 < r_{ij} < 6.0$ Å).

Fragment 1. As mentioned above, in absence of EDTA, this moiety was characterized by dipolar coupling between H28 and both H31 and Me-26. In according to the NOE classifications, these distances were both restrained in the ranges $1.0 < r_{ij} < 3.0$ Å. In order to keep the cation close to the C25−C33 substructure, a very weak distance constraint was used in the calculation. In particular, Ca^{2+} was constrained in the very large range of 1.8−9.0 Å with the two oxygen atoms involved in the ketal functionality at position 33. This served the double purpose of (1) keeping the cation close to the moiety that experimentally had turned out to be mainly affected by its presence and (2) avoiding any bias in the calculations. Thus, the three-dimensional structures of fragment 1 satisfying the NOE constraints were constructed by simulated annealing (SA) calculations. In order to eliminate any possible source of conformational bias, a starting structure of the palytoxin with calcium, characterized by an arbitrary conformation, was minimized. Restrained simulations were carried out for 8 ns using the CVFF force field as implemented in Discover software. The starting point of restrained SA calculations was set at 300 K, and thereafter, the temperature was decreased stepwise down to 100 K. Then, The final step was again constituted by energy-minimization to refine the obtained structures, as reported in the Experimental Section. One hundred structures were generated, and an average RMSD value of 0.000395 ± 0.000222 Å for all heavy atoms was obtained from the superimposition of the 10 lowest energy structures (Figure 4). These data, along with the lack of violations of the experimental restraints, suggested that the

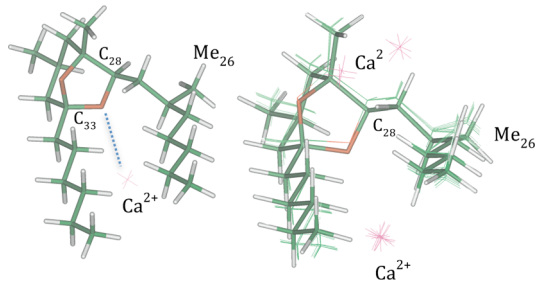

Figure 4. Calculated lowest energy conformer for fragment 1 (left). Superimposition of the top 10 lowest energy conformers for fragment 1 (right).

obtained structures were representative of the structure actually adopted in aqueous solution by palytoxin.

Interestingly, the superimposition of the best structures clearly showed that the structure adopted by the fragment is well-defined and that the Ca^{2+} in 6 out of the 10 best structures is placed in close proximity (approximately at 3.11 Å) of the oxygen bonded to C28 and C33. From a 3D perspective, this is in agreement with the experimental NMR-based observations according to which the C25−C33 segment is mainly affected by the addition of EDTA to the palytoxin sample. It is noteworthy that in three out of four remaining structure the calcium is coordinated by neither oxygen ($3.9 < r_{ij} < 5.5$ Å), while in only one structure (the one with the highest energy) it is coordinated by the oxygen atom connecting C29 with C33 (Figure 4). In conclusion, Ca^{2+} appears to coordinate palytoxin in proximity of the ketal functionality with a preferential coordination bond with the oxygen atom between C28 and C33.

Fragment 2. The conformational study on fragment 2 was performed resorting to the same calculations as for fragment 1. Accordingly, a random conformation of fragment 2 was subjected to restrained SA calculations followed by energy minimization. Distance constraints between H49 and both H50 ($1.0 < r_{ij} < 3.0$ Å) and Me-50 ($2.5 < r_{ij} < 4.5$ Å) and between H52 and H50 ($2.5 < r_{ij} < 4.5$ Å) were adopted. In analogy with the previous calculation, Ca^{2+} was again constrained in a range of 1.8−9.0 Å with respect to the oxygen atom at position 49, on account of our NMR-based evidence.

Average RMSD value of 0.00290 ± 0.00219 Å for all heavy atoms was obtained from the superimposition of the 10 best structures at lowest energy (Figure 5). Also in this case, the structure of the fragment turned out well-defined. The calcium ion adopted a precise location in top 16 lowest energy structures, preferentially coordinating the oxygen atoms at

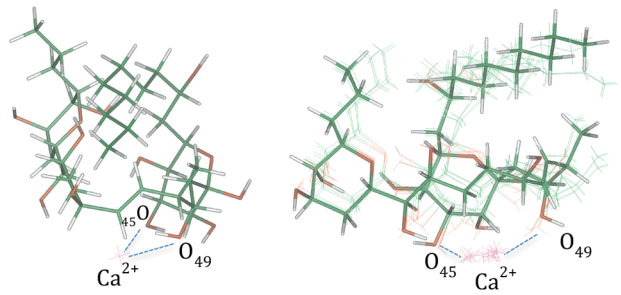

Figure 5. Calculated lowest energy conformer for fragment 2 (left); Superimposition of the top 10 lowest energy conformers for fragment 1 (right).

dx.doi.org/10.1021/jo4022953 | J. Org. Chem. 2014, 79, 72−79

position 49 (in the range of 3.10 Å) and 45 (in the range of 3.35 Å) (Figure 5).

CONCLUSION

Our NMR- and molecular modeling-based study determined that palytoxin is capable of forming complex with calcium ions in aqueous solution. Ca^{2+} is coordinated along the C25−C33 and the C47−C53 palytoxin's part structures. Preferential coordination bonds have been identified between a calcium ion and the ketal oxygen atom linking C28 and C33 as well as between one more calcium ion with oxygen atoms at position 45 and 49, respectively.

Finally, given the importance of calcium in many biological systems and the proven interference of palytoxin with the concentration of cellular cations, including calcium, the study reported herein constitutes a crucial piece of information for those committed to clarifying the toxin bioactivity at a molecular level.

EXPERIMENTAL SECTION

1. Extraction and Isolation of Palytoxin. Palytoxin was extracted from *Palythoa* spp. (purchased from a city aquarium store) according to an experimental procedure set up in our laboratories.[12] The seawater (1000 mL), in which samples of soft corals were immerged, was partitioned against butanol three times. The butanol extract was evaporated and then solubilized in 50 mL of a methanol/water (1:1) solution.

Polyps (8.9 g) were removed from their supporting substrates and immerged in a glass beaker filled with 300 mL of a methanol/water (1:1) solution. The polyps were sonicated three times for 10 min in pulse mode while in an ice bath. The obtained mixture was centrifuged at 5000 g for 20 min and the supernatant evaporated and finally solubilized in 20 mL of a methanol/water (1:1) solution.

This latter solution was combined with the one deriving from the extraction of seawater and partitioned with CH_2Cl_2. The aqueous layer was partly evaporated and the resulting solution (25 mL) loaded onto a 360-g Combiflash C-18 column connected to a Combi*Flash* R_f flash chromatography system. The column was eluted with a H_2O:PrOH solution, whose ratio changed from 60:40 to 10:90 in 50 min. A 45-ml fraction containing palytoxin was collected after 10 min, concentrated and eventually purified on a Gemini 10u HPLC column connected to a SpectraSYSTEM HPLC model P2000, with gradient elution by changing ratios of H_2O:CH_3CN:AcOH from 80:20:01 to 0:100:0.1 in 30 min. Final purification of palytoxin was achieved on a Kinetex 2.6 u HPLC column connected to an Agilent HPLC model 1100 coupled to a linear ion trap LTQ Orbitrap XL hybrid Fourier Transform MS (FTMS) equipped with an ESI ION MAX source. This last purification was carried out by using a 20-min gradient with the same mobile phases as above.

The occurrence of palytoxin in each eluate was ascertained by high-resolution LC/MS analysis in full MS mode (positive ions).

Such extraction and purification procedure eventually afforded 3.2 mg of palytoxin.

2. NMR Experiments. NMR spectra were measured on a Varian Unity Inova 700 spectrometer equipped with a ^{13}C Enhanced HCN Cold Probe. Shigemi 5 mm NMR tubes were used. Chemical shifts are reported in parts per million (ppm) in hertz relative to the solvent peak (d_H 4.67 for HDO; d_H 3.31 and d_C 49.0 for CHD_2OD). Standard Varian pulse sequences were employed for the respective classes of spectra; solvent signal suppression by presaturation was used when required. All NMR data reported in the text were derived from 2D $^1H-^1H$ COSY (sw 5472.0; d1 1.000; nt 240), z-filtered TOCSY (sw 5446.6; d1 1.000; nt 240; mixT 0.080; slpw 34.400; slpwr 42), NOESY (sw 5445.2; d1 1.000; nt 240; three NOESY experiments were recorded using as mixN 0.200, 0.400 and 0.800, respectively), ROESY (sw 5446.3; d1 1.000; nt 240; mixN 0.800), phase-sensitive (ps-) HMBC (sw 5347.6; sw1 33430.8; d1 0.010; nt 160; four HMBC experiments were recorded using as jnxh 4.0, 6.0, 8.0, and 10.0, respectively), and HSQC (sw 5275.7; sw1 28160; j1xh 146.0; d1 1.000; nt 300) spectra. The number of data points was for all of the spectra 2048 × 1024 and it was finally zero-filled to 4096 × 2048.

3. Preparation of Palytoxin−Ca^{2+} Complex. Palytoxin (1,03 mg; 3,85 × 10^{-4} mmol) was dissolved in 5 mL of distilled water. To such solution $CaCl_2$ solubilized in D_2O (8,00 × 10^{-4} mmol; 80 mL) was added and the mixture heated for 2 h. The solvent was then evaporated and the resulting solid further dried in a desiccator overnight. The NMR sample was prepared by adding 500 mL of deuterium oxide (99,8 Atom % D). ^1H NMR, COSY, z-filtered TOCSY, NOESY, ROESY, HSQC, and ps-HMBC were recorded over the next 48 h after the addition of $CaCl_2$. The same NMR spectra were run again after a week and eventually after two weeks.

4. Calcium−EDTA Complex Formation from Palytoxin Natural Sample for NMR Studies. Palytoxin (1,5 mg; 5,6 × 10^{-4} mmol) was dissolved in 500 mL of deuterium oxide (99,8 Atom % D). 1D- and 2D-NMR experiments (^1H NMR, COSY, z-filtered TOCSY, NOESY, ROESY, HSQC, and ps-HMBC) were carried out. To such solution 8 equivalents of EDTA solubilized in D_2O was added (80 mL) and the mixture heated for 2 h. ^1H NMR, COSY, z-filtered TOCSY, NOESY, ROESY, HSQC, and ps-HMBC were recorded over the next 48 h following the addition of EDTA. The same NMR spectra were run again after a week and eventually after two weeks.

5. Structure Calculations on Palytoxin−Ca^{2+} Complex. Cross-peak volume integrations were performed with the program iNMR,[13] using the NOESY experiment collected at mixing time of 800 ms. The NOE volumes were then converted to distance restraints, after they were calibrated using known fixed distance (H98/H99; 2.42 Å). Then a NOE restraint file was generated with three distance classifications as follows: strong NOEs ($1.0 < r_{ij} < 3.0$ Å), medium NOEs ($2.5 < r_{ij} < 4.5$ Å) and weak NOEs ($4.0 < r_{ij} < 6.0$ Å).

The calculations have been performed using a distance-dependent macroscopic dielectric constant of 4*r* and an infinite cutoff for non bonded interactions to partially compensate for the lack of the solvent have been used.[14] Thus, the 3D structures satisfying NOE constraints were constructed by simulated annealing calculations. An initial structure of both fragment 1 (from position 21 through 39) and fragment 2 (from position 33 to 65) were built using a completely random array of atoms. Using the steepest descent followed by the quasi-Newton−Raphson method (VA09A), the conformational energy was minimized. Restrained simulations were carried out for 8 ns using the CVFF force field as implemented in Discover software. The simulation started at 300 K, and then the temperature was decreased stepwise until 100 K. The final step was again constituted by energy-minimization to refine the obtained structures. This was performed through using successively the steepest descent and the quasi-Newton−Raphson (VA09A) algorithms. Both dynamics and mechanics calculations were carried out by using 10 kcal mol^{-1} $Å^{-2}$ flatwell distance restraints for all proton−proton distances, while 1 kcal mol^{-1} $Å^{-2}$ flatwell distance restraints was used for calcium cation. In both calculations (fragments 1 and 2), 100 structures were generated. RMSD (root-mean-square deviation) value of 0.000395 ± 0.000222 Å and 0.00290 ± 0.00219 Å for heavy atoms was calculated for the best ten structures for fragments 1 and 2, respectively. Illustrations of structures were generated using the Insight II.

ASSOCIATED CONTENT

Supporting Information

NMR spectra of palytoxin in CD_3OD: ^1H NMR, COSY, z-filtered TOCSY, ROESY, HSQC, HMBC; NMR spectra of palytoxin in D_2O: ^1H NMR, z-filtered TOCSY, ROESY, NOESY, HSQC, HMBC; NMR spectra of palytoxin added with 8 equiv of EDTA in D_2O: ^1H NMR, z-filtered TOCSY, ROESY, and NOESY together with key enlargements of some 2D homo- and heteronuclear experiments. This material is available free of charge via the Internet at http://pubs.acs.org.

dx.doi.org/10.1021/jo4022953 | J. Org. Chem. 2014, 79, 72−79

AUTHOR INFORMATION

Corresponding Author

*e-mail: forino@unina.it.

Notes

The authors declare no competing financial interest.

ACKNOWLEDGMENTS

This work was supported by the Italian Ministry of Education University and Research (PRIN 2009JS5YX9_002).

REFERENCES

(1) Moore, R. E.; Scheuer, P. J. *Science (Washington, D.C.)* **1971**, *172*, 495−498.
(2) Wu, C. H. *Toxicon* **2009**, *54*, 1183−1189.
(3) Rossini, G. P.; Bigiani, A. *Toxicon* **2011**, *57*, 429−439.
(4) Bottinger, H.; Beress, L.; Habermann, E. *Biochim. Biophys. Acta* **1986**, *861*, 165−176.
(5) Artigas, P.; Gadsby, D. C. *J. Gen. Physiol.* **2004**, *123*, 357−376.
(6) Schilling, W. P.; Snyder, D.; Sinkins, W. G.; Estacion, M. *Am. J. Physiol. Cell Physiol.* **2006**, *291*, C657−C667.
(7) Ciminiello, P.; Dell'Aversano, C.; Dello Iacovo, E.; Fattorusso, E.; Forino, M.; Grauso, L.; Tartaglione, L. *J. Am. Soc. Mass Spectrom.* **2012**, *23*, 952−963.
(8) Kan, Y.; Uemura, D.; Hirata, Y.; Ishiguro, M.; Iwashita, T. *Tetrahedron Lett.* **2001**, *42*, 3197−3202.
(9) Moore, R. E.; Bartolini, G.; Barchi, J.; Bothner-By, A. A.; Dadok, J.; Ford, J. *J. Am. Chem. Soc.* **1982**, *104*, 3776−3779.
(10) Inuzuka, T.; Uemura, D.; Arimoto, H. *Tetrahedron* **2008**, *64*, 7718−7723.
(11) Inuzuka, T.; Fujisawa, T.; Arimoto, H.; Uemura, D. *Org. Biomol. Chem.* **2007**, *5*, 897−899.
(12) Ciminiello, P.; Dell'Aversano, C.; Dello Iacovo, E.; Fattorusso, E.; Forino, M.; Grauso, L.; Tartaglione, L.; Guerrini, F.; Pezzolesi, L.; Pistocchi, R.; Vanucci, S. *J. Am. Chem. Soc.* **2012**, *134*, 1869−1875.
(13) www.iNMR.net (accessed November 15, 2013).
(14) Weiner, S. J.; Kollman, P. A.; Case, D. A.; Singh, U. C.; Ghio, C.; Alagona, G.; Profeta, S.; Weimer, P. *J. Am. Chem. Soc.* **1984**, *106*, 765−784.